ISSN 1330-3651
UDC/UDK 620.191.33:539.42

APPLICATION OF THE Δ*K*, Δ*J* AND Δ*CTOD* PARAMETERS IN FATIGUE CRACK GROWTH MODELLING

Željko Božić, Marijo Mlikota, Siegfried Schmauder

Subject review

This paper presents the developed fatigue crack growth models based on parameters Δ*K*, Δ*J*-integral and Δ*CTOD* determined by using linear elastic and elastic plastic FE analysis. The fatigue crack growth threshold values of the considered crack growth driving force parameters, below which crack propagation does not occur, were taken into account. Fatigue crack growth tests with constant load amplitude were carried out on a centrally cracked plate specimen until collapse occurred. The tests were performed on mild steel specimens at room temperature in laboratory air, at a loading frequency of 5 Hz. For the analyzed specimen, the calculated Δ*J*-integral range values obtained *by* linear elastic analysis, ΔJ_{le}, and the elastic-plastic values, ΔJ_{ep}, were close at lower crack growth rates. As the crack length increases the ΔJ_{ep} values became higher as compared with the linear elastic values, ΔJ_{le}, This indicates that small scale yielding conditions prevailed only for smaller crack lengths. The models based on the EPFM parameters ΔJ_{ep} and Δ*CTOD* provide better agreement with experimental results for higher crack growth rates, compared with the models based on the LEFM parameters Δ*K* and ΔJ_{le}.

Keywords: *CTOD, EPFM, fatigue crack growth, J-integral, LEFM*

Primjena Δ*K*, Δ*J* i Δ*CTOD* parametara u modeliranju rasta zamornih pukotina

Pregledni članak

U radu su izloženi modeli rasta zamornih pukotina, temeljeni na parametrima mehanike loma Δ*K*, Δ*J*-integral i Δ*CTOD* koji su utvrđeni koristeći linearno elastičnu i elasto-plastičnu analizu metodom konačnih elemenata. Prag napredovanja pukotine, koji predstavlja graničnu vrijednost relevantnog parametra mehanike loma ispod koje ne dolazi do napredovanja pukotine, uzet je u obzir u modelima. Proveden je test zamora s konstantnom amplitudom cikličkog rasteznog opterećenja za uzorak ploče sa središnjom pukotinom. Test je proveden za uzorak od mekog konstrukcijskog čelika u laboratoriju na sobnoj temperaturi s frekvencijom 5 Hz. Za manje duljine pukotine vrijednosti izračunate u linearno elastičnoj analizi ΔJ_{le} poklapaju se s ΔJ_{ep} vrijednostima izračunatim u elasto-plastičnoj analizi. Za veće duljine pukotina parametar ΔJ_{ep} raste brže od linearno elastičnog parametra ΔJ_{le}, što pokazuje da je pretpostavka linearno elastične mehanike loma o malim plastičnim deformacijama u ligamentu zadovoljena samo za manje duljine pukotine. Modeli temeljeni na elasto-plastičnim parametrima ΔJ_{ep} i Δ*CTOD* daju bolje slaganje simuliranog životnog vijeka s eksperimentalnim rezultatima nego linearno elastični modeli temeljeni na parametrima Δ*K* i ΔJ_{le}.

Ključne riječi: *CTOD, EPML, J-integral, LEML, rast pukotine uslijed zamora*

1 Introduction
Uvod

The fatigue life of a structural component is usually split into a crack initiation period and a crack growth period, [1, 2]. Nucleation of micro cracks generally occurs very early in the fatigue life. The initiation period is supposed to include some micro crack growth or short crack growth, [3, 4]. At this stage the fatigue cracks are still too small to be visible. After some micro crack growth has occurred away from the nucleation site, a more regular growth is observed, [5]. This is the beginning of the so-called long crack growth period. At this stage, the crack is growing in a stable manner until failure occurs. Various stages in the fatigue life are given in Fig. 1.

It is technically significant to consider the crack initiation and stable crack growth periods separately. Crack length of 1mm represents a limit between the short and long cracks, [6, 7]. This length is also considered as a limit size in NDT inspections. Once cracks become visible, the remaining fatigue life of a structural component is usually a smaller part of the total life. This part is particularly important for the fail-safe and safe-life designs of structures such as aircrafts, ships, etc. [2].

For the two periods the fatigue prediction methods are different. The stress concentration factor K_t is the important parameter for predictions on crack initiation. Analysis of crack initiation period is usually based on Palmgren-Miner's linear cumulative damage hypothesis, [8, 9]. For prediction of fatigue crack growth the fracture mechanics parameters such as Stress Intensity Factor (SIF), *K, J*-integral and Crack Tip Opening Displacement (*CTOD*), δ, are considered as a crack driving force.

The fatigue crack growth prediction models are fracture mechanics based models that have been developed to support the damage tolerance concepts in metallic structures. The common approach to fatigue crack growth analysis is to describe the data by a differential equation, which is referred to as a fatigue crack growth law or model. By integrating the equation one can obtain the crack length versus number of cycles, *a*-*N* curve, and predict the number of cycles required for the crack to grow from an initial to the final size.

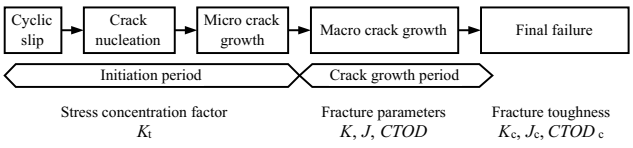

Figure 1 *Stages in the fatigue life*
Slika 1. *Stadiji kod zamora*

There are different criteria for crack growth considering the brittle or ductile behaviour of the material. Linear Elastic Fracture Mechanics assumption (LEFM) usually dominates in brittle materials and the crack growth criterion is described by SIF *K*. Ductile materials are often based on Elastic

Plastic Fracture Mechanics (EPFM) assumption and different parameters such as energy release rate, *G*, *J*-integral, or *CTOD*, δ, represent the crack propagation criterion. It is necessary to mention that crack growth criterion for ductile materials is also valid for brittle materials. [28]

The fatigue crack growth is in essence brittle and it is often based on LEFM assumptions. The well-known Paris law is based on the stress intensity factor range ΔK, which represents the difference of the maximum and minimum K value, $\Delta K = K_{max} - K_{min}$, associated with the maximum and minimum applied nominal stress in a loading cycle, σ_{min} and σ_{max}, respectively, [10]. The Paris equation (1) does not take account of the effect of loading ratio, i.e. $R = \sigma_{min}/\sigma_{max}$. It is well-known from experimental observations that R-ratio affects the rate of crack growth [1]. As a consequence, C_p and m_p also vary in relation to the R-ratio changes. Walker [11] and Forman [12] extended Paris' model by taking account of the stress ratio R. The Forman equation can also describe higher crack growth rates, da/dN, when K_{max} approaches to the fracture toughness value, K_{Ic}. The fracture toughness value, K_{Ic}, is a critical K_I value associated with fracture onset and it represents a material property.

$$\frac{da}{dN} = C_p(\Delta K)^{m_p}. \quad (1)$$

Growth of long cracks may take place if the applied cyclic stress is high enough to provide the SIF range higher than the stress intensity factor range threshold ΔK_{th}, [6, 7]. Its value is determined experimentally by using the decreasing K test as described in the ASTM E647 document.

There are cases when LEFM does not govern fatigue crack growth rate. Some examples are: short crack growth, crack growth in welded areas, low cycle fatigue, crack growth under large scale yielding regime, etc. In such cases the EPFM parameters *J*-integral and CTOD can be considered as a crack driving force. Dowling and Begley [13] suggested implementation of Δ*J*-integral for fatigue crack growth modelling under large scale yielding conditions. Branco et al. [14] investigated fatigue crack growth under tensile cyclic loading using mild steel specimens and concluded that crack growth rate at higher strains is substantially controlled by Δ*J*-integral. Chow and Lu [15] discussed implementation of the Δ*J*-integral to crack growth rate modelling under small and large scale yielding. In reference [16] is presented a crack growth model based on Δ*J*-integral, by means of which crack growth rates for two different steels were examined. McEvily [30] proposed a model that relates the crack growth rate to the crack tip opening displacement and includes the threshold effect.

This paper presents results of calculated fracture mechanics parameters SIF, *K,* *J*-integral and *CTOD*, δ, by using Linear Elastic (LE) and Elastic Plastic (EP) FE analysis, for a centrally cracked plate specimen. A fatigue test with constant load amplitude was carried out on the centrally cracked plate specimen. The material used for the specimens is conventional mild steel for welded structures. In the experiment higher crack growth rates were observed in the last part of the specimen's total fatigue life.

The calculated *J*-integral values obtained by LE and EP analysis are close initially, for shorter crack lengths, and for longer cracks the EP values are higher as compared with the LE values. This suggested that the specimen was not under small scale yielding during the whole fatigue life, which is in agreement with higher crack growth rates observed in the experiment when the crack became longer. Crack growth models based on parameters Δ*K*, Δ*J* and Δ*CTOD* are developed in order to simulate fatigue crack growth life for the test specimen.

2
Fatigue crack growth models
Modeli rasta zamornih pukotina

In a structure subjected to a cyclic load, a fatigue crack nucleus can be initiated on a microscopically small scale. The initiated crack grows further to a macroscopic size, and finally the component fails in the last cycle of the fatigue life. A typical fatigue crack growth rate curve, commonly called a da/dN versus ΔK curve, is illustrated in Fig. 2. The curve is defined by Regions A, B and C which is commonly referred to as region I, II and III respectively, [31].

Region I represents the early development of a fatigue crack and the crack growth rate; da/dN is typically of the order 10^{-9} m/cycle or smaller. This region is highly influenced by the crack growth threshold, ΔK_{th}, below which long fatigue cracks practically do not propagate. Region II represents the intermediate crack propagation zone where the length of the plastic zone ahead of the crack tip is long compared with the mean grain size, but much smaller than the crack length. The use of LEFM concepts is acceptable and the data follows a linear relationship between log da/dN and log ΔK. The crack growth rate is typically on the order of 10^{-9} to 10^{-6} m/cycle. The influence of the mean stress is probably the most significant and usually results in closely spaced lines parallel to each other. This region corresponds to stable crack growth.

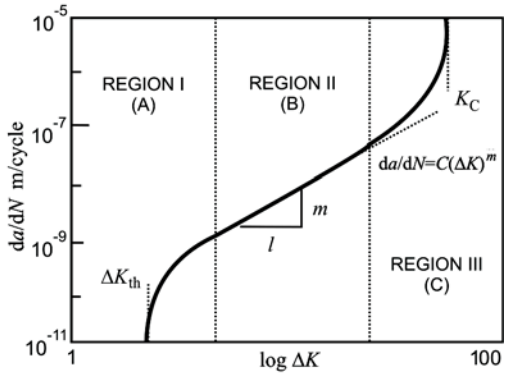

Figure 2 *Fatigue rate curve*
Slika 2. *Krivulja rasta zamora*

Region III represents the fatigue crack growth at very high rates, da/d$N > 10^{-6}$ m/cycle associated with a rapid and unstable crack growth just prior to final failure. The corresponding stress level is very high and causes a large plastic zone near the crack tip. Because large scale yielding occurs, the influence of the nonlinear properties of the material cannot be ignored. The use of LEFM is not entirely correct and nonlinear fracture mechanics should be applied to this stage.

Various fatigue crack growth prediction models have been developed to analyze propagation of long cracks. Paris used ΔK parameter to explain FCGR behaviour based on the LEFM assumption. For situations of fatigue crack growth under large scale yielding regime, where the stress intensity factor is no longer valid, Dowling and Begley introduced

a model with ΔJ-integral as the crack driving force parameter, Eq. (2).

$$\frac{\mathrm{d}a}{\mathrm{d}N} = C_{\mathrm{db}} (\Delta J)^{m_{\mathrm{db}}}. \tag{2}$$

Where C_{db} and m_{db} are the constants of the Dowling-Begley equation and $\Delta J = J_{\max} - J_{\min}$, is the J-integral range. In LEFM the parameters K and J-integral are correlated. Assuming the plane stress conditions, the following correlation exists:

$$J = \frac{K^2}{E}, \tag{3}$$

where E is Young's modulus. From the equations (1), (2) and (3), the constants m_{db} and C_{db} are given by (4) and (5).

$$m_{\mathrm{db}} = \frac{m_{\mathrm{p}}}{2}, \tag{4}$$

$$C_{\mathrm{db}} = E^{\frac{m_{\mathrm{p}}}{2}} \cdot C_{\mathrm{p}}. \tag{5}$$

McEvily proposed a crack growth models based on the crack tip opening displacement range, $\Delta CTOD$. A crack growth model based on $\Delta CTOD = CTOD_{\max} - CTOD_{\min}$, is given by equation (6).

$$\frac{\mathrm{d}a}{\mathrm{d}N} = C_{\mathrm{ctod}} (\Delta CTOD)^{m_{\mathrm{ctod}}}. \tag{6}$$

Elastic Plastic Fracture Mechanics gives relationship between the CTOD and J-integral:

$$\Delta CTOD = d_{\mathrm{n}} \cdot \frac{J}{\sigma_{\mathrm{Y}}}, \tag{7}$$

where σ_{Y} is yield stress and d_{n} is a correlation parameter which depends on material properties.

For a crack growth model given by Eq. (6), and by means of Eqs. (2) and (7) the constants C_{ctod} and m_{ctod} are given by Eqs. (8) i (9).

$$m_{\mathrm{ctod}} = m_{\mathrm{db}}, \tag{8}$$

$$C_{\mathrm{ctod}} = \left(\frac{1}{d_{\mathrm{n}}} \cdot \sigma_{\mathrm{ty}} \right)^{m_{\mathrm{db}}} \cdot C_{\mathrm{db}}. \tag{9}$$

The threshold stress intensity factor range value, ΔK_{th}, is a ΔK value bellow which crack growth practically does not occur, [17, 18]. Paris' equation does not take account of the threshold ΔK_{th}. In a crack growth model the threshold stress intensity factor range, ΔK_{th}, can be taken into account considering the effective part of the SIF range ΔK_{eff}, as given by the Eq. (10).

$$\Delta K_{\mathrm{eff}} = \Delta L - \Delta K_{\mathrm{th}}. \tag{10}$$

In LEFM the correlation between ΔK_{th} and ΔJ_{th} is given by the Eq. (11).

$$\Delta J_{\mathrm{th}} = \frac{\Delta K_{\mathrm{th}}}{E \cdot (2\Delta K - \Delta K_{\mathrm{th}})}. \tag{11}$$

In accordance with Eq. (7), the correlation between ΔJ_{th} and $\Delta CTOD_{\mathrm{th}}$ can be represented by the Eq. (12).

$$\Delta CTOD_{\mathrm{th}} = d_{\mathrm{n}} \cdot \frac{\Delta J_{\mathrm{th}}}{E}. \tag{12}$$

The crack growth models (1), (2) and (6) do not take into account the fatigue threshold parameters (10), (11) and (12). In this work the fatigue threshold parameters ΔK_{th} and ΔJ_{th} and $\Delta CTOD_{\mathrm{th}}$ are considered in the implemented crack growth models.

An extension of the Paris equation (1) based on the effective stress intensity factor range, ΔK_{eff}, (10) is given by (13). This equation is also known as the Zheng-Hirt model, [19].

$$\frac{\mathrm{d}a}{\mathrm{d}N} = C_{\mathrm{peff}} \cdot (\Delta K_{\mathrm{eff}})^{m_{\mathrm{peff}}} = C_{\mathrm{peff}} \cdot (\Delta K - \Delta K_{\mathrm{th}})^{m_{\mathrm{peff}}}. \tag{13}$$

The modified Dowling and Begley model (2) which takes account of the J-integral threshold, ΔJ_{th}, is represented by Eq. (14).

$$\frac{\mathrm{d}a}{\mathrm{d}N} = C_{\mathrm{db_{eff}}} \cdot (\Delta J_{\mathrm{eff}})^{m_{\mathrm{db_{eff}}}} = C_{\mathrm{db_{eff}}} \cdot (\Delta J - \Delta J_{\mathrm{th}})^{m_{\mathrm{db_{eff}}}}. \tag{14}$$

The crack growth model based on $\Delta CTOD$ parameter, which includes threshold $\Delta CTOD_{\mathrm{th}}$ values, is represented by Eq. (15).

$$\frac{\mathrm{d}a}{\mathrm{d}N} = C_{\mathrm{ctod_{eff}}} \cdot (\Delta CTOD_{\mathrm{eff}})^{m_{\mathrm{ctod_{eff}}}} = C_{\mathrm{ctod_{eff}}} \cdot (\Delta CTOD - \Delta CTOD_{\mathrm{th}})^{m_{\mathrm{ctod_{eff}}}}. \tag{15}$$

Considering the Paris equation (1), the number of constant amplitude loading cycles due to which a crack grows from an initial crack length, a_0, to a final crack length, a_{fin}, can be determined by the integration of the equation (16).

$$N = \int_{a_0}^{a_{\mathrm{fin}}} \frac{\mathrm{d}a}{C[\Delta K_{\mathrm{I}}]^m}. \tag{16}$$

The integration of the Paris equation (16) can be performed numerically. For discrete crack lengths, a, the SIF values are calculated by FEA. Between the two discrete SIF values, a linear interpolation is used. The segmental crack growth life, ΔN, between the two discrete crack lengths, a and $a+\Delta a$, is calculated by equation (17).

$$\Delta N = \int_{a}^{a+\Delta a} \frac{\mathrm{d}a}{C[\Delta K_{\mathrm{I}}(a)]^m}. \tag{17}$$

The total fatigue life of a specimen is calculated as a sum of segmental fatigue lives, $\Sigma \Delta N$. For the other crack growth equations the integration is performed in a similar manner.

3
Experimental results of fatigue crack growth in a centrally cracked plate
Eksperimentalni rezultati rasta pukotine u ploči sa središnjom pukotinom

By using a hydraulic fatigue testing machine a plate specimen with a central crack was exposed to constant amplitude cyclic tension load until failure occurred, [20]. The specimen geometry is shown in Fig. 3.

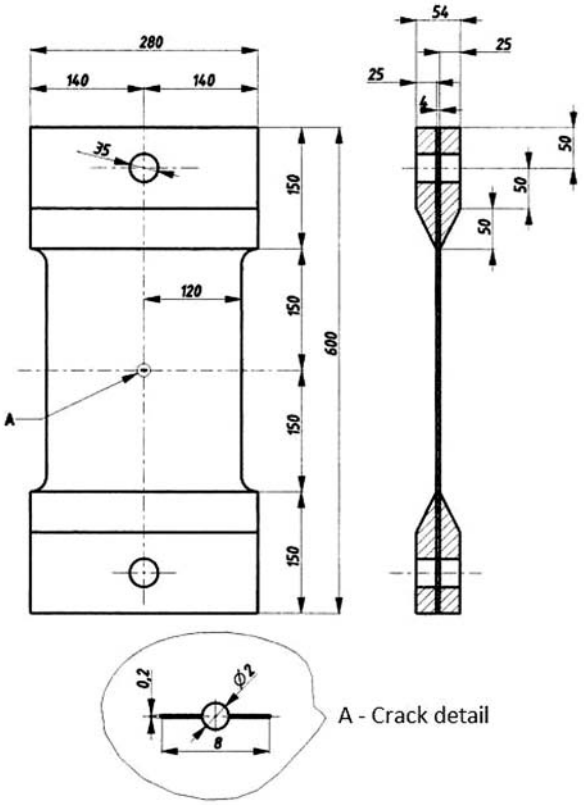

Figure 3 *Fatigue test specimen*
Slika 3. *Uzorak za ispitivanje zamora*

Fatigue test conditions applied in the experiment are given in Tab. 1. The applied average stress range related to a cross-section in the intact area was $\Delta\sigma_o$ = 80 MPa. The loading frequency was 5 Hz. The force range and the stress ratio are denoted by $\Delta F = F_{max} - F_{min}$ and $R = F_{min}/F_{max}$, respectively. The initial notch length was $2a$ = 8 mm. The material used for the specimens is conventional mild steel for welded structures with the material properties specified in Tab. 2.

Table 1 *Loading conditions and geometry characteristics of the fatigue test specimen*
Tablica 1. *Uvjeti opterećenja i karakteristike geometrije uzorka za ispitivanje zamora*

ΔF/N	A_o /mm^2	$\Delta\sigma_o$ /MPa	R
76800	960	80	0,0253

Crack length data presented here were measured by using an optical microscope. Obtained crack length values, a, with respect to the number of applied loading cycles, N, are given in the a-N diagram shown in Fig. 4. The measured crack lengths represent the averaged half crack lengths. The crack lengths given in Fig. 4, start from the first measured values in the experiment.

Table 2 *Material properties of the specimen*
Tablica 2. *Svojstva materijala uzorka*

Yield strength	235 MPa
Tensile strength	≥ 400 MPa
Elastic modulus	206 GPa
Poisson ratio	0,3

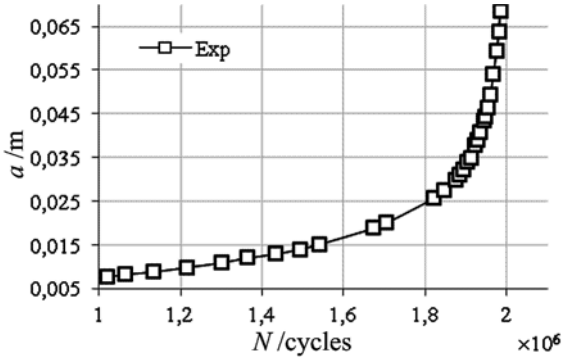

Figure 4 *Experimentally determined fatigue life curve, a-N.*
Slika 4. *Eksperimentalno utvrđena krivulja zamora a-N*

It is to observe that the crack propagated at a higher growth rate after a crack length of 30 mm up to a final crack length ≈ 80 mm, where rapid and unstable crack propagation took place prior to the final failure.

4
Numerical determination of the *K* and *J*-integral and CTOD parameters
Numeričko utvrđivanje parametara *K*, *J*-integral i CTOD

Fracture mechanics uses concepts from applied mechanics to develop an understanding of the stress and deformation fields around a crack tip when a crack is present in a structure. A sound knowledge of these stress and deformation fields helps in calculating fracture mechanics parameters which together with fatigue crack growth models enable developing fail-safe and safe-life designs for structures such as aerospace, shipbuilding, nuclear, civil, and mechanical engineering.

In this section is discussed numerical determination of fracture mechanics parameters such as the SIF, *K, J-integral and the Crack Tip Opening Displacement, CTOD*, by using FE software, [29].

In order to discretize the specimen geometry the second order 8-node plane stress elements PLANE183 is employed. Owning to the double-symmetry only one quarter of the specimen is modelled. The typical FE mesh of the centrally notched specimen, with applied symmetry boundary conditions is given in Fig. 5.

The SIF, *K, is normally* determined in a linear elastic FE analysis. In the FEM modelling the crack tip region is meshed by singular elements. The procedure for the calculation of SIFs is based on the application of well-known "quarter-point" elements introduced by Barsoum, [21]. Barsoum showed that the proper crack tip displacement and the stress and strain fields are modelled by standard quadratic order isoparametric finite elements if one simply moves the element mid-side node to the position one quarter of the way from the crack tip to the far end of the element. This procedure introduces a singularity into the mapping between the element's parametric coordinate space and Cartesian space.

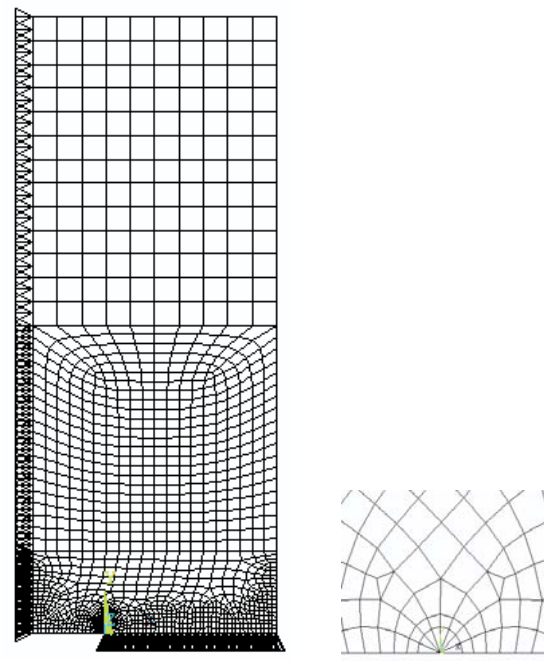

Figure 5 *The finite element mesh model of the centrally notched plate specimen: a) model of one quarter of the specimen, b) the crack tip region.*
Slika 5. *Model mreže konačnog elementa centralno zarezanog uzorka: a) model jedne četvrtine uzorka, b) područje vrha pukotine*

The *J*-integral, in its simplest form, can be defined as a path-independent line integral that measures the strength of the singular stresses and strains near a crack tip. The magnitude of *J*-integral has been evaluated using the expression suggested by Rice [22].

$$J = \int_{\Gamma} W \mathrm{d}y - \int \left(t_x \cdot \frac{\delta u_x}{\delta x} + t_y \cdot \frac{\delta u_y}{\delta y} \right) \mathrm{d}s. \qquad (18)$$

In the equation the meaning of the used symbols is as follows: Γ – any path surrounding the crack tip, W – strain energy density, $\boldsymbol{t}_i = \boldsymbol{\sigma}_{ij} \cdot \boldsymbol{n}_j$ – traction vector, σ – component stress, n – unit outer normal vector to path Γ, u_i – displacement vector, s – distance along the path Γ. The *J*-integral contour path surrounding a crack-tip is illustrated in Fig. 6.

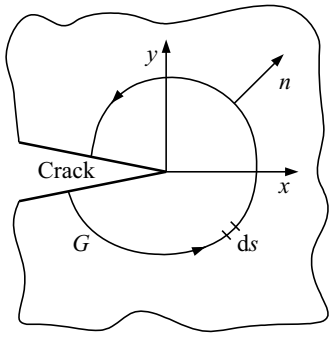

Figure 6 *J-integral contour path surrounding a crack-tip*
Slika 6. *Putanje konture J-integrala oko vrha pukotine*

It was observed in the analysis, that there exists some deviation between the magnitudes of estimated Δ*J* values for the paths to close to the crack tip, due to numerical accuracy. Hence, Δ*J* has been calculated over 14 different contours around the crack tip, as shown in Fig. 7. It is observed that the Δ*J* reaches a stabilized value by getting slightly far from the crack tip. In other words, they are independent of path. The mean value of the calculated Δ*J* parameters was determined, considering the stabilized values.

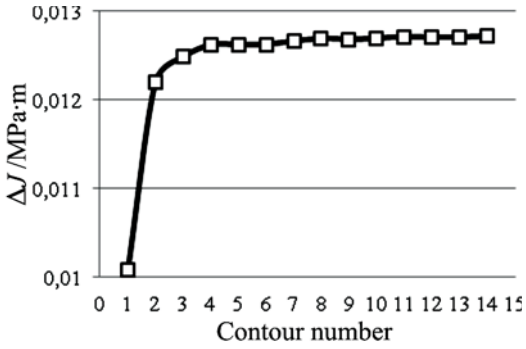

Figure 7 *J-integral values stabilize with distance increase of the contour path from the crack tip*
Slika 7. *Vrijednosti J-integrala stabiliziraju se porastom udaljenosti putanje konture od vrha pukotine*

The magnitudes of *CTOD* for various crack lengths are estimated by 90°-intercept method introduced by Rice [22], as shown in Fig. 8.

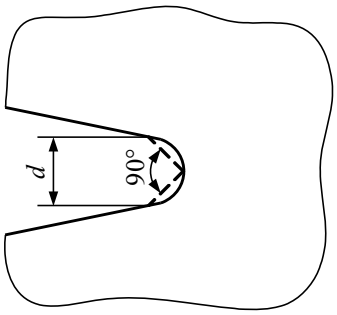

Figure 8 *Definition of the CTOD parameter, δ*
Slika 8. *Definicija parametra CTOD, δ*

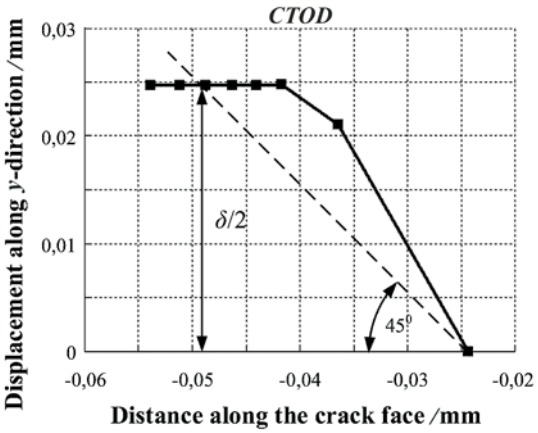

Figure 9 *Estimation of the CTOD by 90° intercepts method for the specific crack length, a ≈ 68,5 mm*
Slika 9. *Procjena CTOD-a metodom 90° segmenta pravca za specifičnu duljinu pukotine, a ≈ 68,5 mm.*

For an analyzed crack length, the displacement of each node along the crack face is listed with the help of ANSYS post processor [29] and plotted using graphic software. Such a typical plot for a central notched specimen for the specific value of crack length is shown in Fig. 9. The intercept of y-displacement of crack face with the 45° lines

drawn from the crack-tip is taken as half part of a *CTOD* value.

Linear elastic and elastic-plastic FE analysis was carried out for the considered specimen, assuming the same loading conditions as implemented in the experiment. The material properties used in the numerical model correspond to those given in Tab. 2. For elastic-plastic FE analysis the material behaviour has been considered to be bilinear isotropic hardening type pertaining to the mild steel as given in Fig. 10. Once static analysis is completed, the general postprocessor is used to calculate fracture mechanics parameters, [29].

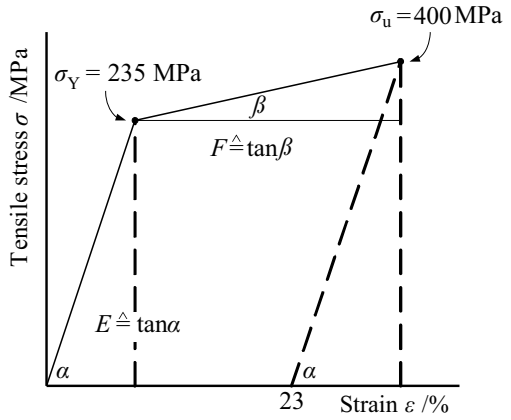

Figure 10 *Bilinear isotropic hardening material characteristic*
Slika 10. *Karakteristika bilinearnog izotropnog očvršćivanja materijala*

5
Results and discussion
Rezultati i diskusija

The Mode I stress intensity factors, K_I, were determined for the considered specimen by using linear elastic analysis, as described in the previous section. The calculated stress intensity factor range values, ΔK_I, with respect to the half crack length are given in Fig. 11.

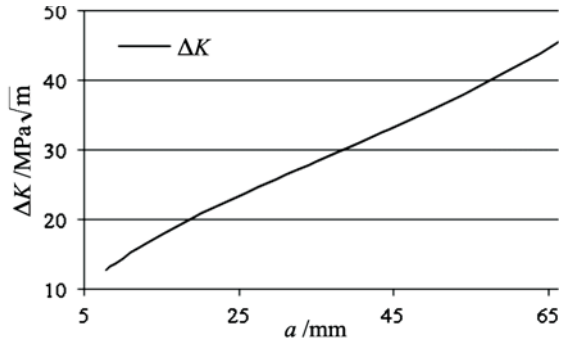

Figure 11 *Calculated stress intensity factors as a function of crack length.*
Slika 11. *Izračunati faktori intenziteta naprezanja kao funkcija duljine pukotine*

Δ*J*-integral range was calculated based on both, the LEFM and EPFM assumptions. Fig. 12 shows the Δ*J* –integral range values with respect to crack length, obtained by the LE analysis, ΔJ_{LE}, and the EP analysis, ΔJ_{EP}. Threshold ΔJ_{th} values are illustrated in the figure as well. Initially, up to a half crack length $a \approx 30$ mm, the calculated values in the LE and EP analysis give close results and for longer cracks ΔJ_{EP} values calculated in the EP analysis

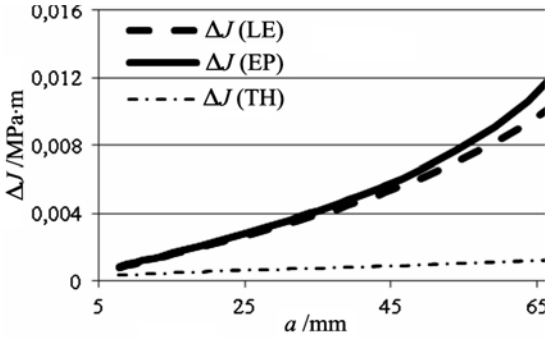

Figure 12 *ΔJ-integral range values calculated by using the LE and EP analysis and threshold values*
Slika 12. *Vrijednosti raspona ΔJ-integrala korištenjem analize LE I EP i graničnih vrijednosti*

increase faster. This indicates that small scale yielding conditions prevail only for smaller crack lengths and for longer cracks a larger plastic zone occurs. Fig. 13 shows the values of the calculated Δ*CTOD* as a function of the crack length, obtained by using an EP FE analysis. The threshold $\Delta CTOD_{th}$ values are given in the figure as well.

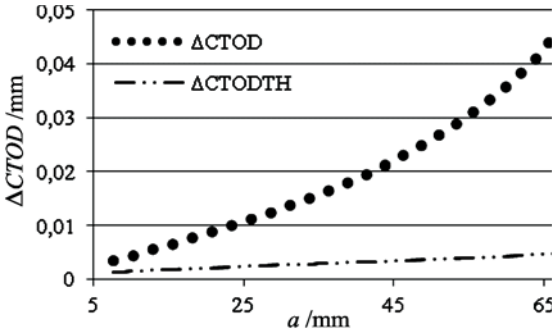

Figure 13 *Values of ΔCTOD and $\Delta CTOD_{th}$ as a function of crack length*
Slika 13. *ΔCTOD i $\Delta CTOD_{th}$ vrijednosti u funkciji duljine pukotine*

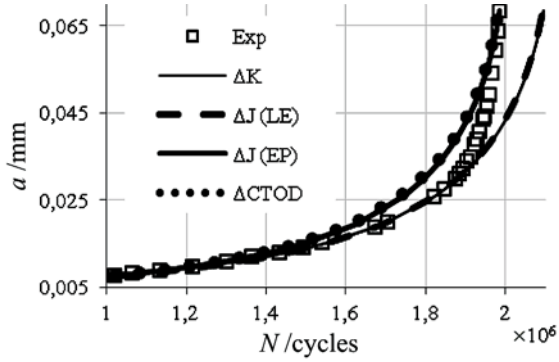

Figure 14 *Simulated fatigue life curves in comparison with experimental results*
Slika 14. *Simulirane krivulje životnog vijeka u usporedbi s eksperimentalnim rezultatima*

The integration of models has been performed by using MATLAB software. For the LE model (13) the threshold stress intensity range is constant and is equal to: $\Delta K_{th} = 2{,}9$ MPa$\sqrt{\text{m}}$, [23]. The constants of the crack growth model are: $C_p = 1{,}43\times10^{-11}$ and $m_p = 2{,}75$. The units for Δ*K* and d*a*/d*N* are MPa$\sqrt{\text{m}}$ and m, respectively. For modified Dowling and Begley model, represented by Eq. (14), the crack growth model parameters are taken as $C_{db} = 2{,}8967\times10^{-4}$, $m_{db} = 1{,}375$. The units for Δ*J* and d*a*/d*N* are MPa·m and m, respectively. The integration is performed for the model taking into account the values ΔJ_{LE} and ΔJ_{EP}, and threshold

values ΔJ_{th} given in Fig. 12. For the model given by (15) the integration is performed using the Δ*CTOD* and threshold $\Delta CTOD_{th}$ values given in Fig. 13. For this model the crack growth parameters are: $C_{ctod} = 0{,}6012$ and $m_{ctod} = 1{,}375$. The units for Δ*CTOD* and d*a*/d*N* are m and m, respectively. Fig. 14 shows the simulated fatigue life curves for the considered models in comparison to the experimental fatigue life curve.

Linear elastic analysis models based on the parameters Δ*K* and ΔJ_{LE} provide identical fatigue life curves. The models provide a very good agreement with experiential data up to a crack length $a \approx 30$ mm. However, these models predict a slower crack growth in the last part of the total fatigue life, and provide a too long fatigue life, compared to experimental results. The elastic-plastic analysis based models, with the parameters ΔJ_{EP} and Δ*CTOD*, provided very close fatigue life curves, where the simulated fatigue life is slightly shorter compared with the experiment.

6
Conclusion
Zaključak

Fatigue crack growth test on a mild steel centrally cracked plate specimen subjected to constant load amplitude showed high crack growth rates in the last part of the specimen's total fatigue life. Crack growth models which take LEFM parameters Δ*K* and ΔJ_{LE}, and EPFM parameters ΔJ_{EP} and Δ*CTOD* as a crack driving force, were developed in order to simulate fatigue crack growth life for the test specimen. The calculated ΔJ_{LE} and ΔJ_{EP} values obtained by linear elastic and elastic plastic FE analysis, respectively, are close initially, for shorter crack lengths. For longer cracks the ΔJ_{EP} values are higher as compared with the ΔJ_{LE} values. Initially, for shorter crack lengths small scale yielding conditions prevailed, and for longer cracks a larger plastic zone occurs. The LE models predicted a slower crack growth in the last part of the total fatigue life, and provided a too long fatigue life, compared to experimental results. The models based on EPFM parameters ΔJ_{EP} and Δ*CTOD* provided better agreement with experimental results for higher crack growth rates, compared with the LEFM models based on parameters Δ*K* and ΔJ_{LE}.

7
References
Literatura

[1] Broek, D. The Practical Use of Fracture Mechanics. Kluwer Academic Publishers, Dordrecht, 1988.

[2] Schijve, J. Fatigue of Structures and Materials. Springer Science+Business Media, B. V., 2009.

[3] Santus C., Taylor D. Physically short crack propagation in metals during high cycle fatigue. // International Journal of Fatigue, 31, 8(2009), 1356–1365.

[4] Schijve, J. Fatigue of structures and materials in the 20th century and the state of the art. // International Journal of Fatigue, 25, 1(2003), 679-702.

[5] Schijve, J.; Campoli, G.; Monaco, A. Fatigue of aircraft materials and structures. // International Journal of Fatigue, 16, 1(1994), 21-32.

[6] Vasudevan, A. K.; Sadananda, K.; Glinka, G. Critical parameters for fatigue damage. // International Journal of Fatigue, 23, 1(2001), 39–54.

[7] Sadananda, K.; Vasudevan, A. K. Crack tip driving forces and crack growth representation under fatigue, International Journal of Fatigue, 25, (2003), 899–914.

[8] Palmgren, A. The endurance of ball bearings. Z. Ver Deut Ing, 68, (1923), 339-341.

[9] Miner, M. A. Cumulative damage in fatigue. Journal of Applied Mechanics, 12, (1945), 159–164.

[10] Paris, P.; Erdogan, F. A critical analysis of crack propagation laws. Journal of Basic Engineering, 85, (1963), 528–534.

[11] Walker, E. K. The effect of stress ratio during crack propagation and fatigue for 2024-T3 and 7076-T6 aluminum. In: Effect of environment and complex load history on fatigue life. ASTM STP 462. Philadelphia: American Society for Testing and Materials, 1970.,1–14.

[12] Forman, R. G. Study of fatigue crack initiation from flaws using fracture mechanics theory. Engineering Fracture Mechanics, 4, 2(1972), 333–345.

[13] Dowling, N. E.; Begley J. A. Fatigue crack growth during gross plasticity and the J-integral. Mechanics of Crack Growth. ASTM STP 590, American Society for Testing and Materials, Philadelphia, PA, 1976., 82-105.

[14] Branco, C. M.; Radon, J. C.; Culver, L. E. Elastic-plastic fatigue crack growth under load cycling. // The Journal of Strain Analysis for Engineering Design, 12, 2(1977), 71-80.

[15] Chow, C. L.; Lu, T. J. On the Cyclic J-integral Applied to Fatigue Cracking. // International Journal of Fracture, 40, 1989., 53–59.

[16] Gasiak, G.; Rozumek, D. Δ*J*-integral range estimation for fatigue crack growth rate description. // International Journal of Fatigue, 26, 2(2004), 135–140.

[17] Liu, Y.; Mahadevan, S. Threshold stress intensity factor and crack growth rate prediction under mixed-mode loading. // Engineering Fracture Mechanics, 74, (2007), 332–345.

[18] Pook, L. P. The fatigue crack direction and threshold behavior of mild steel under mixed-mode I and III loading. // International Journal of Fatigue, 7, (1985), 21–30.

[19] Zheng, X.; Hirt, M. A. Fatigue crack propagation in steels. // Engineering Fracture Mechanics, 18, 5(1983), 965–973.

[20] Sumi, Y.; Bozic, Z.; Iyama, H.; Kawamura, Y. Multiple Fatigue Cracks Propagating in a Stiffened Panel. // Journal of the Society of Naval Architects of Japan, 179, (1996), 407-412.

[21] Barsoum, R. Further application of quadratic isoparametric elements to linear fracture mechanics of plate bending and general shells. // International Journal for Numerical Methods in Engineering, 11, (1976), 167-169.

[22] Rice, J. R. A Path Independent Integral and the Approximate Analysis of Strain Concentration by Notches and Cracks. // Journal of Applied Mechanics, 35, (1968), 379–386.

[23] Okawa, T.; Sumi, Y.; Mohri, M. Simulation-based fatigue crack management of ship structural details applied to longitudinal and transverse connections. // Marine Structures, 19, (2006).

[24] Shih, C. F. Relationship between the J-integral and the Crack Tip Opening Displacement for Stationary and Extending Cracks. // Journal of the Mechanics and Physics of Solids, 29, (1981), 305–326.

[25] Klesnil, M.; Lukáš, P. Fatigue of metallic materials. Materials Science Monographs, 7, 1980.

[26] Tada, H.; Paris, P. C.; Irwin, G.R. The Stress Analysis of Cracks Handbook. American Society of Mechanical Engineers, 2000.

[27] Božić, Ž.; Wolf, H.; Semenski, D. Fatigue Growth of Multiple Cracks in Plates under Cyclic Tension. // Transactions of FAMENA, 34, 1(2010), 1 – 12.

[28] Shahani, A. R.; Moayeri Kashani, H.; Rastegar, M.; Botshekanan Dehkordi, M. A unified model for the fatigue crack growth rate in variable stress ratio, Fatigue & Fracture of Engineering Materials & Structures, 32, 2(2009), 105-118.

[29] Swanson Analysis System, Inc. ANSYS User's Manual Revision 11.0, 2009.

[30] McEvily, A. J. Phenomenological and Microstructural Aspects of Fatigue. Presented at the Third International Conference on the Strength of Metals and Alloys, Cambridge, England; published by the Institute and The Iron and Steel Institutes, Publication, W33, 1974., 204-213.
[31] Beden¸ S. M.; Abdullah, S.; Ariffin, A. K. Review of Fatigue Crack Propagation Models for Metallic Components // European Journal of Scientific Research. The Web version (2009).
URL:http://www.eurojournals.com/ejsr.htm. (21.12.2010.).
URL:http://onlinelibrary.wiley.com/journal/10.1111/%28ISSN%291460-2695. (21.12.2010.).

Authors' addresses
Adrese autora

Željko Božić, PhD, Professor
Deptartment of Aeronautical Engineering
Faculty of Mechanical Engineering and Naval Architecture
University of Zagreb
Ivana Lucica 5, HR-10000 Zagreb, Croatia
Tel.: +385-(0)1-6168 536
Fax.: +385-(0)1-6156 940
Email: zeljko.bozic@fsb.hr

Marijo Mlikota, Mag. Ing. Mech.
Faculty of Mechanical Engineering and Naval Architecture
University of Zagreb
Ivana Lucica 5, HR-10000 Zagreb, Croatia
Email: marijo.mlikota@fsb.hr

Siegfried Schmauder, Prof. Dr. rer. nat.
Institute for Materials Testing, Materials Science
and Strength of Materials (IMWF)
University of Stuttgart
Pfaffenwaldring 32, D-70569 Stuttgart, Germany
Tel.: 0711/685-62556
Fax: 0711/685-62635
Email: siegfried.schmauder@imwf.uni-stuttgart.de